

Evolution of electronic structure from insulator to superconductor in $\text{Bi}_2\text{Sr}_{2-x}\text{La}_x(\text{Ca}, \text{Y})\text{Cu}_2\text{O}_{8+\delta}$

K. Tanaka,¹ T. Yoshida,¹ K. M. Shen,^{2,3} D. H. Lu,² W. S. Lee,² H. Yagi,¹ A. Fujimori,¹ Z.-X. Shen,² Risdiana,⁴ T. Fujii,^{4,5} and I. Terasaki⁴

¹*Department of Physics, University of Tokyo, Hongo, Tokyo 113-0033, Japan*

²*Department of Applied Physics and Stanford Synchrotron Radiation Laboratory, Stanford University, Stanford, California 94305, USA*

³*Department of Physics, Laboratory of Atomic and Solid State Physics, Cornell University, Ithaca, New York 14853, USA*

⁴*Department of Applied Physics, Waseda University, Tokyo 169-8555, Japan*

⁵*Cryogenic Center, University of Tokyo, Bunkyo-ku, Tokyo 113-0032, Japan*

(Received 11 August 2009; published 16 March 2010)

La-doped and Y-doped $\text{Bi}_2\text{Sr}_2\text{CaCu}_2\text{O}_{8+\delta}$ compounds $\text{Bi}_2\text{Sr}_{2-x}\text{La}_x(\text{Ca}, \text{Y})\text{Cu}_2\text{O}_{8+\delta}$, which range from the insulator to the deeply underdoped superconductor, have been studied by angle-resolved photoemission spectroscopy. We have observed that the lower Hubbard band (LHB) of the parent insulator is gradually shifted upward with doping without significantly changing the band dispersions, which implies a downward shift of the chemical potential with hole doping. This behavior is analogous to $\text{Bi}_2\text{Sr}_{2-x}\text{La}_x\text{CuO}_{6+\delta}$ and $\text{Ca}_{2-x}\text{Na}_x\text{CuO}_2\text{Cl}_2$ but is different from $\text{La}_{2-x}\text{Sr}_x\text{CuO}_4$, where the LHB stays well below the chemical potential and does not move while its intensity quickly diminishes in the underdoped region.

DOI: 10.1103/PhysRevB.81.125115

PACS number(s): 74.72.-h, 79.60.-i, 71.30.+h

I. INTRODUCTION

The question of how the electronic structure of high- T_c cuprates evolves from the Mott insulator to the superconductor with hole doping is one of the most fundamental and important issues in condensed-matter physics. This subject has been extensively investigated experimentally and theoretically but still remains highly controversial. Previous angle-resolved photoemission spectroscopy (ARPES) studies have revealed two different cases. In underdoped $\text{La}_{2-x}\text{Sr}_x\text{CuO}_4$ (LSCO), a “two-component” electronic structure has been observed, that is, upon hole doping “in-gap” states appear primarily well (~ 0.4 eV) above the lower Hubbard band (LHB), the chemical potential does not shift and spectral weight is transferred from the LHB to the in-gap states for further hole doping within the underdoped region.^{1–3} Already in the lightly doped region, a weak quasiparticle (QP) peak crosses the Fermi level (E_F) in the $(0,0)$ - (π,π) nodal direction and is responsible for the metallic transport.² ARPES spectra of underdoped $\text{Ca}_{2-x}\text{Na}_x\text{CuO}_2\text{Cl}_2$ (Na-CCOC)⁴ and $\text{Bi}_2\text{Sr}_{2-x}\text{La}_x\text{CuO}_{6+\delta}$ (Bi2201),⁵ on the other hand, show that upon hole doping the chemical potential moves to the top of the LHB and continues to shift downward for further hole doping.

As for the $\text{Bi}_2\text{Sr}_2\text{CaCu}_2\text{O}_{8+\delta}$ (Bi2212) family, the apparently smooth evolution of ARPES spectra in the $(\pi,0)$ region in a combined plot of undoped $\text{Ca}_2\text{CuO}_2\text{Cl}_2$ (CCOC) and underdoped Bi2212 implies that a behavior similar to Na-CCOC is expected for Bi2212.⁶ A core-level photoemission study of Bi2212 has indeed shown that the chemical potential is shifted with doping in underdoped samples⁷ unlike LSCO. Recently, a momentum distribution curve (MDC) analysis of Bi2201⁵ and underdoped Na-CCOC⁸ have revealed the existence of an additional QP band just above the LHB crossing E_F . Here, strong electron-phonon interaction has been proposed to result in the dressed coherent QP band accompanied by a high-energy incoherent (Frank-Condon-type) feature. Yet, the different behavior of the chemical-

potential shift and the LHB-QP energy separation between LSCO and Na-CCOC or Bi2201 remains to be explained. In order to see what makes those differences between the different families in the evolution of the electronic structure from the Mott insulator to the superconductor, we have performed detailed ARPES measurements of lightly doped Bi2212.

II. EXPERIMENTS

Recently, high-quality crystals of lightly doped Bi2212 have become available,⁹ which enabled us to study the systematic doping dependence covering from the insulator to the superconductor. In particular, substituting La for the Sr site instead of substituting for the Ca site has made lightly doped Bi2212 samples metallic ($dp/dT > 0$) in an analogous way to the lightly doped LSCO¹⁰ and $\text{YBa}_2\text{Cu}_3\text{O}_{7-\delta}$ (YBCO).¹¹ Single crystals of $\text{Bi}_2\text{Sr}_{2-x}\text{La}_x\text{CaCu}_2\text{O}_{8+\delta}$ and $\text{Bi}_2\text{Sr}_2\text{Ca}_{0.8}\text{Y}_{0.2}\text{Cu}_2\text{O}_{8+\delta}$ were grown by the traveling solvent floating-zone method. X-ray diffraction showed no trace of impurity phases. Details of the sample preparation are given elsewhere.⁹ The hole concentration p per Cu atom was determined using the empirical relationship between p and the room-temperature thermopower.¹² All the samples show metallic transport at 300 K while some of them show insulating behavior ($dp/dT < 0$) at low temperatures. p , T_c , T_{\min} , and ρ_{\min} of the measured samples are listed in Table I. Here, T_{\min} is the temperature at which the resistivity reaches the minimum value ρ_{\min} . The $\text{Bi}_2\text{Sr}_2\text{Ca}_{0.8}\text{Y}_{0.2}\text{Cu}_2\text{O}_{8+\delta}$ ($p=0.075$) sample was superconducting and above T_c $dp/dT > 0$.

ARPES measurements were carried out at beamline 5-4 of Stanford Synchrotron Radiation Laboratory (SSRL). Incident photons had an energy of $h\nu=19$ eV. A Scienta SES-200 analyzer was used in the angle mode with the total energy and momentum resolution of ~ 14 meV and $\sim 0.3^\circ$, respectively. Samples were cleaved *in situ* under an ultrahigh vacuum of 10^{-11} Torr and measured at ~ 10 K. The position of the Fermi level was calibrated with gold spectra.

TABLE I. Chemical compositions, hole concentration p , T_c , T_{\min} , and ρ_{\min} of Bi2212 samples studied in the present work.

$\text{Bi}_2\text{Sr}_{2-x}\text{La}_x\text{CaCu}_2\text{O}_{8+\delta}$	p	T_c (K)	T_{\min} (K)	ρ_{\min} (m Ω cm)
$x=0.8$	0.03	-	150	5
$x=0.7$	0.05	-	130	3.2
$x=0.6$	0.06	-	-	-
$\text{Bi}_2\text{Sr}_2\text{Ca}_{0.8}\text{Y}_{0.2}\text{Cu}_2\text{O}_{8+\delta}$	0.075	30	-	-

III. RESULTS AND DISCUSSION

Figures 1(a)–1(d) shows energy distribution curves (EDCs) along the diagonal $k=(0,0)$ – (π,π) direction (nodal direction) in the second Brillouin zone (BZ). The intensity maps in E - k space shown in Figs. 1(e)–1(h) reveal the peak dispersion. First, the spectra for $p=0.03$ show a single dispersive peak marked by “MB (main band)” plus a diffraction replica marked by “SS” due to the Bi-O plane superstructure. This peak disperses closest to E_F around $\sim(\pi/2, \pi/2)$, and can be considered as a remnant of the LHB or more precisely of the Zhang-Rice singlet band. With hole doping p , the dispersive peak as a whole moves upward until an obvious E_F crossing in the nodal direction occurs for $p \sim 0.075$, where the system becomes superconducting. This is contrasted with spectra of LSCO with similar doping levels, where the LHB stays away (~ -0.5 eV) from E_F but a sharp QP peak crossing E_F is visible already for $p \approx 0.03$ ² due to the presence of two separate spectral features, namely, the LHB and the QP crossing E_F .

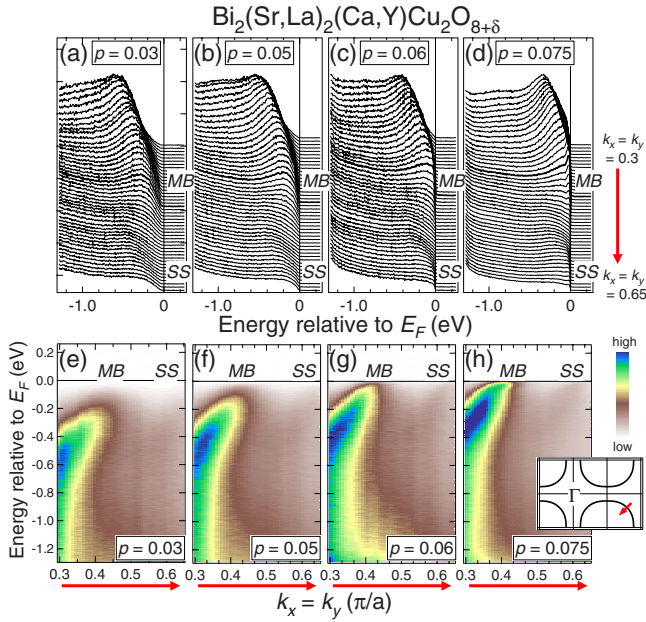


FIG. 1. (Color online) ARPES spectra of lightly doped Bi2212 along the $(0,0)$ – (π,π) nodal direction in the second BZ. [(a)–(d)]: EDCs. A bold line for each doping indicates the spectrum where the dispersive feature comes closest to E_F . [(e)–(h)]: intensity plot of the spectra in the E - k plane. The features denoted by SS are diffraction replica of the MB due to the Bi-O plane superstructure.

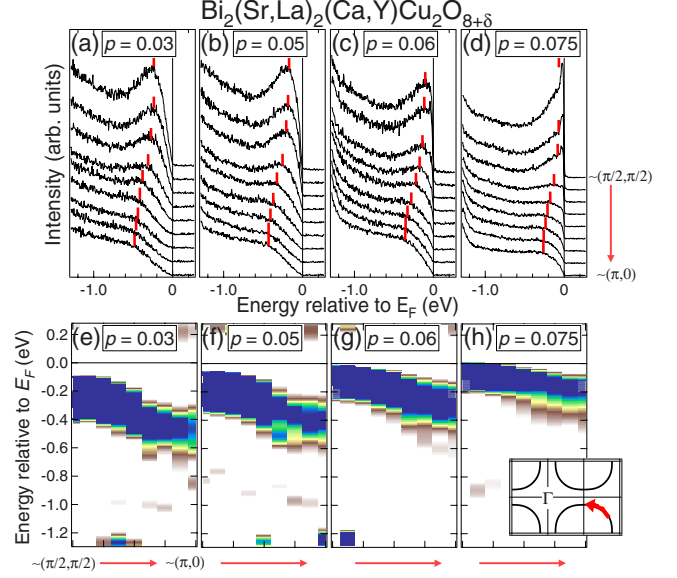


FIG. 2. (Color online) ARPES spectra of lightly doped Bi2212 along the underlying Fermi surface in the second BZ. [(a)–(d)]: EDCs. The peak position determined by the second derivatives are shown by vertical bars. [(e)–(h)]: second derivatives of the EDCs in the E - k plane.

Figures 2(a)–2(d) shows the ARPES spectra along the “underlying” Fermi surface.⁶ Here, by the underlying Fermi surface is meant the minimum-gap locus including the pseudogap region around $k \approx (\pi, 0)$ as reported for underdoped Bi2212.¹³ The figure again shows a single dispersive feature that moves upward with hole doping p . This is also contrasted with the case of LSCO where the LHB stays ~ 0.5 eV below E_F , where the QP crosses, leading to the two-component behavior, in particular, around $(\pi, 0)$.¹¹ While a dispersive peak which crosses E_F occurs in the $(0,0)$ – (π,π) nodal direction (for $p \geq 0.075$), no E_F crossing occurs and a finite (pseudo)gap persists around $k \sim (\pi, 0)$. The second derivatives of the spectra shown in Figs. 2(e)–2(h) indicate the dispersion along the underlying Fermi surface.

In Fig. 3, we have plotted the doping dependence of the peak positions in EDCs on the (underlying) Fermi surface at

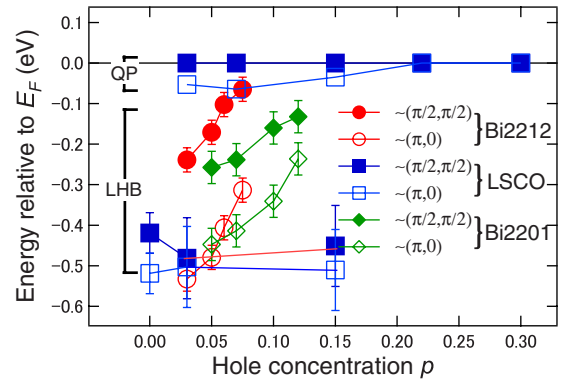


FIG. 3. (Color online) Energy positions of the EDC peaks at $\sim(\pi/2, \pi/2)$ and $\sim(\pi, 0)$ in Bi2212, LSCO¹⁴, and Bi2201⁵ as functions of doping levels.

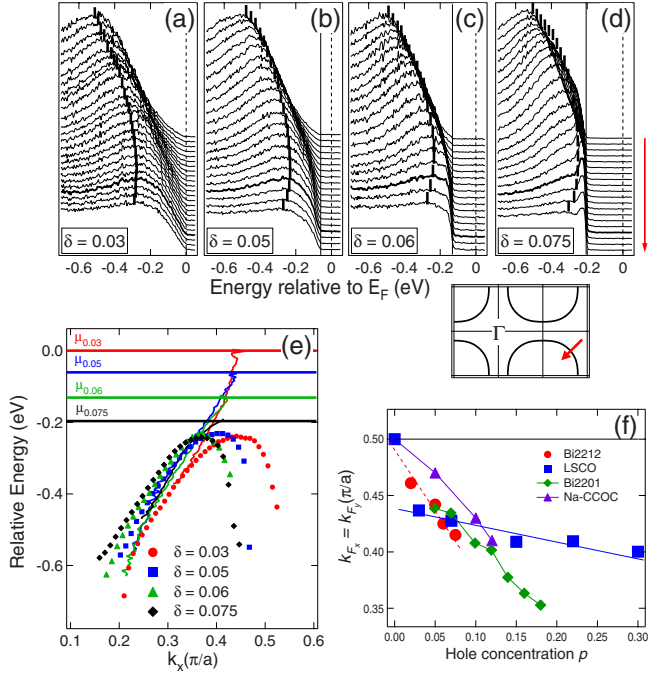


FIG. 4. (Color online) Doping evolution of the electronic structure along the nodal direction near E_F . [(a)–(d)]: blow up of Fig. 1 near E_F . Vertical bars indicate the position of the LHB. (e): position of the LHB and the “QP” band obtained from MDCs. The plots have been shifted vertically so that the chemical potential μ shifts the average of the shift in the LHB at $\sim(\pi/2, \pi/2)$ and $\sim(\pi, 0)$ in Fig. 3 for each doping. The chemical potential μ is also displayed. (f): doping dependence of Fermi momentum k_F positions in Bi2212, LSCO¹⁴, Bi2201⁵, and Na-CCOC⁸.

$\sim(\pi/2, \pi/2)$ and those at $\sim(\pi, 0)$ thus determined by taking the second derivatives. One can see that in Bi2212, the peak positions at $\sim(\pi/2, \pi/2)$ and $\sim(\pi, 0)$ show nearly parallel shifts with doping in the lightly doped region, again indicating a rigid-bandlike shift of the LHB similar to the case of Na-CCOC⁸ and Bi2201.⁵ In the same figure, we have plotted the doping dependence of the peak position at $\sim(\pi/2, \pi/2)$ and $\sim(\pi, 0)$ in LSCO determined in the same way.¹⁴ In LSCO, a sharp QP feature appears near E_F already at $p \sim 0.03$ and stays there while the LHB is located at ~ -0.5 eV. The amount of the shift of each feature is much smaller in LSCO than that in Bi2212 and Na-CCOC.

To reveal further details of the evolution of the electronic structure near E_F , EDCs along $(0,0)$ – (π, π) of lightly doped Bi2212 are plotted on an expanded scale in Figs. 4(a)–4(d) with the peak positions determined by the second derivatives of the EDCs. Figure 4(e) shows the dispersion of the EDC peak (representing that of the LHB) along the $(0,0)$ – (π, π) direction. In addition, we have plotted the dispersion of the “QP band” which has been determined by the MDC analysis, as performed for Bi2201⁵ and Na-CCOC.⁸ Although there is no sharp peak crossing E_F in the EDCs of the $p=0.03$ and 0.05 samples, the peak in the MDCs shows a clear dispersion crossing E_F , as shown in Fig. 4(e). Here, the results for each composition have been shifted so that the LHB positions coincide. One can see that the chemical potential thus obtained is shifted downward relative to the LHB with hole

doping. One can also see that the valence-band maximum of the LHB is shifted in k space from $\sim(\pi/2, \pi/2)$ toward $(0,0)$ with hole doping. Remarkably, the QP band stays almost at the same position in the E – k space in this plot and the E_F crossing point, namely, k_F in the nodal direction is shifted toward $(0,0)$ following the downward chemical potential with hole doping. From Figs. 1–4 one can conclude that the lightly doped Bi2212 shows a rigid-bandlike shift of the LHB [except for the small shift toward $k \sim (0,0)$] and the nodal QP just above the LHB, analogous to the case of Bi2201 and Na-CCOC. This behavior is different from LSCO, where the LHB stays almost at the same energy and the clear QP band is seen well (~ -0.5 eV) above the LHB.

In the antiferromagnetic (AF) insulating state of the undoped compound, the maximum of the LHB along the nodal direction should occur on the AF zone boundary, that is, exactly at $(\pi/2, \pi/2)$ due to the folding of the BZ in the AF state. Without the long-range order, on the other hand, k_F can, in principle, take any value. Therefore, it is interesting to see how the k_F evolves as a function of p . In order to see this, we have plotted in Fig. 4(f) the doping dependence of the k_F position determined from the MDC peak position at E_F as a function of p . One can see from the figure that the LHB in lightly doped Bi2212 indeed moves toward $(\pi/2, \pi/2)$ with decreasing hole concentration. The results for Na-CCOC ($p=0, 0.05, 0.1, 0.12$) also showed the same behavior.⁸ On the other hand, k_F in LSCO extrapolates to $\sim(0.44\pi, 0.44\pi)$ and not to $(\pi/2, \pi/2)$ until $p \approx 0.03$. [For undoped La_2CuO_4 , a tiny amount of holes are doped due to excess oxygen and faint E_F spectral weight appears at $(\pi/2, \pi/2)$]. This can be understood as due to the separated features of the LHB and the QP band crossing E_F in LSCO. This observation again points to the similarity between Bi2212, Bi2201, and Na-CCOC concerning the evolution of the electronic structure.

From the present data, one can also obtain an important implication for the doping dependence of spectra across the insulator-superconductor transition (between $p=0.06$ and 0.075) in Bi2212. Nodal spectra in the superconducting phase ($p=0.075$) have a sharp QP peak around E_F without a gap whereas nodal spectra in the insulating phase ($p=0.06$) have finite shoulderlike spectral weight (weak and broad QP peak) around E_F with a ~ 9 meV leading-edge gap. It therefore appears that the system shows superconductivity when the nodal spectra show a sharp QP peak crossing E_F . This behavior is consistent with the recently proposed two-gap scenario^{15,16} that superconductivity occurs in the nodal region in underdoped samples. Our observation indeed implies a close relationship between the occurrence of superconductivity and the existence of QP peak around the node. Here, it should be noted again that one can observe a nodal QP peak already for $p \approx 0.03$ in the insulating LSCO. Thus, it seems that the doping evolution of the electronic structure is whether a QP feature appears near E_F well above the LHB before a significant chemical-potential shift occurs or not. So far, LSCO has been the only example that shows the appearance of a QP band before the chemical potential starts to shift in the lightly doped region. It is an important question to ask which makes this difference between the different families of cuprates. It has been pointed out that the major difference in

the electronic structure of the CuO_2 plane between LSCO and Bi2212 lies in the magnitude of the next-nearest-neighbor hopping t' within the single band description of the CuO_2 plane.^{17,18} The magnitude of t' is expected to decrease with influence of the apical oxygen on the CuO_2 plane,¹⁸ and therefore LSCO, which has the shortest Cu-apical oxygen distance among these cuprate families, is expected to have the smallest $|t'|$. According to the t - t' - t'' - J model calculation, a larger energy shift of the chemical potential with hole doping in the underdoped region has been predicted for larger $|t'|$,¹⁹ consistent with our observation that Bi2212 and Na-CCOC showed faster chemical-potential shift than LSCO.

Recently, the new interpretation of the ARPES line shapes of undoped and lightly doped cuprates in Na-CCOC and LSCO was proposed,^{8,20,21} which took into account polaronic effects because arising from strong electron-phonon coupling. The broad hump structure was successfully explained by polaronic effects. The similarity of the spectral line shape between lightly doped Bi2212 and Na-CCOC indicates that the polaronic scenario can also be applied to Bi2212, too. Moreover, theoretical works reported that the phase separation, which occurs with suitable electron-phonon coupling strength,²² successfully explained the doping evolution of the electronic structure of underdoped LSCO, namely, the two-component behavior.²³ The calculation also predicted that phase separation would be suppressed when the electron-phonon coupling becomes stronger and the system shows polaronic insulating state.²² This implies that Bi2212, Bi2201, and Na-CCOC have larger electron-phonon interaction than LSCO and the different strength of electron-phonon

coupling makes different doping evolution of the electronic structure in the different families of cuprates.

IV. SUMMARY

We have observed the evolution of the electronic structure with hole doping in lightly doped Bi2212 from the insulator (with high-temperature metallic behavior) to the superconductor. The results show rigid-bandlike shifts of (the remnant of) the LHB with hole doping. The chemical potential is shifted downward and a QP feature appears around E_F just above the LHB. This evolution of the electronic structure, together with the shift of the momentum position of the maximum of the LHB, are similar to those reported for Bi2201 and Na-CCOC but are different from LSCO. In order to establish whether the different t' 's and different strength of electron-phonon coupling are responsible for the different doping evolution of LSCO and Bi2212, systematic studies on other cuprate families as well as further theoretical studies are desired.

ACKNOWLEDGMENTS

We acknowledge technical help by N. P. Armitage. This work was supported by a grant-in-Aid for Scientific Research in Priority Area "Invention of Anomalous Quantum Materials" (Grant No. 16076208) from MEXT, Japan. SSRL is operated by the DOE Office of Basic Energy Science Divisions of Chemical Sciences and Material Sciences.

¹A. Ino, C. Kim, M. Nakamura, T. Yoshida, T. Mizokawa, Z.-X. Shen, A. Fujimori, T. Kakeshita, H. Eisaki, and S. Uchida, *Phys. Rev. B* **62**, 4137 (2000).

²T. Yoshida, X. J. Zhou, T. Sasagawa, W. L. Yang, P. V. Bogdanov, A. Lanzara, Z. Hussain, T. Mizokawa, A. Fujimori, H. Eisaki, Z.-X. Shen, T. Kakeshita, and S. Uchida, *Phys. Rev. Lett.* **91**, 027001 (2003).

³A. Ino, T. Mizokawa, A. Fujimori, K. Tamasaku, H. Eisaki, S. Uchida, T. Kimura, T. Sasagawa, and K. Kishio, *Phys. Rev. Lett.* **79**, 2101 (1997).

⁴F. Ronning, T. Sasagawa, Y. Kohsaka, K. M. Shen, A. Damascelli, C. Kim, T. Yoshida, N. P. Armitage, D. H. Lu, D. L. Feng, L. L. Miller, H. Takagi, and Z.-X. Shen, *Phys. Rev. B* **67**, 165101 (2003).

⁵M. Hashimoto, T. Yoshida, H. Yagi, M. Takizawa, A. Fujimori, M. Kubota, K. Ono, K. Tanaka, D. H. Lu, Z.-X. Shen, S. Ono, and Yoichi Ando, *Phys. Rev. B* **77**, 094516 (2008).

⁶F. Ronning, C. Kim, D. L. Feng, D. S. Marshall, A. G. Loeser, L. L. Miller, J. N. Eckstein, I. Bozovic, and Z.-X. Shen, *Science* **282**, 2067 (1998).

⁷N. Harima, A. Fujimori, T. Sugaya, and I. Terasaki, *Phys. Rev. B* **67**, 172501 (2003).

⁸K. M. Shen, F. Ronning, D. H. Lu, W. S. Lee, N. J. C. Ingle, W. Meevasana, F. Baumberger, A. Damascelli, N. P. Armitage, L. L. Miller, Y. Kohsaka, M. Azuma, M. Takano, H. Takagi, and Z.-X.

Shen, *Phys. Rev. Lett.* **93**, 267002 (2004).

⁹T. Fujii and I. Terasaki, *Physica C* **392-396**, 238 (2003).

¹⁰Y. Ando, A. N. Lavrov, S. Komiya, K. Segawa, and X. F. Sun, *Phys. Rev. Lett.* **87**, 017001 (2001).

¹¹Y. Ando, A. N. Lavrov, and K. Segawa, *Phys. Rev. Lett.* **83**, 2813 (1999).

¹²S. D. Obertelli, J. R. Cooper, and J. L. Tallon, *Phys. Rev. B* **46**, 14928 (1992).

¹³H. Ding, M. R. Norman, T. Yokoya, T. Takeuchi, M. Randeria, J. C. Campuzano, T. Takahashi, T. Mochiku, and K. Kadowaki, *Phys. Rev. Lett.* **78**, 2628 (1997).

¹⁴A. Ino, C. Kim, M. Nakamura, T. Yoshida, T. Mizokawa, A. Fujimori, Z.-X. Shen, T. Kakeshita, H. Eisaki, and S. Uchida, *Phys. Rev. B* **65**, 094504 (2002); T. Yoshida, X. J. Zhou, K. Tanaka, W. L. Yang, Z. Hussain, Z.-X. Shen, A. Fujimori, S. Sahrakorpi, M. Lindroos, R. S. Markiewicz, A. Bansil, Seiki Komiya, Yoichi Ando, H. Eisaki, T. Kakeshita, and S. Uchida, *ibid.* **74**, 224510 (2006).

¹⁵K. Tanaka, W. S. Lee, D. H. Lu, A. Fujimori, T. Fujii, Risdiana, I. Terasaki, D. J. Scalapino, T. P. Devereaux, Z. Hussain, and Z.-X. Shen, *Science* **314**, 1910 (2006).

¹⁶M. Hashimoto, T. Yoshida, K. Tanaka, A. Fujimori, M. Okusawa, S. Wakimoto, K. Yamada, T. Kakeshita, H. Eisaki, and S. Uchida, *Phys. Rev. B* **75**, 140503(R) (2007).

¹⁷K. Tanaka, T. Yoshida, A. Fujimori, D. H. Lu, Z.-X. Shen, X.-J.

- Zhou, H. Eisaki, Z. Hussain, S. Uchida, Y. Aiura, K. Ono, T. Sugaya, T. Mizuno, and I. Terasaki, Phys. Rev. B **70**, 092503 (2004); C. T. Shih, T. K. Lee, R. Eder, C.-Y. Mou, and Y. C. Chen, Phys. Rev. Lett. **92**, 227002 (2004).
- ¹⁸E. Pavarini, I. Dasgupta, T. Saha-Dasgupta, O. Jepsen, and O. K. Andersen, Phys. Rev. Lett. **87**, 047003 (2001).
- ¹⁹T. Tohyama and S. Maekawa, Phys. Rev. B **67**, 092509 (2003).
- ²⁰O. Rösch, O. Gunnarsson, X. J. Zhou, T. Yoshida, T. Sasagawa, A. Fujimori, Z. Hussain, Z.-X. Shen, and S. Uchida, Phys. Rev. Lett. **95**, 227002 (2005).
- ²¹A. S. Mishchenko and N. Nagaosa, Phys. Rev. Lett. **93**, 036402 (2004).
- ²²M. Capone, G. Sangiovanni, C. Castellani, C. Di Castro, and M. Grilli, Phys. Rev. Lett. **92**, 106401 (2004).
- ²³M. Mayr, G. Alvarez, A. Moreo, and E. Dagotto, Phys. Rev. B **73**, 014509 (2006); G. Alvarez, M. Mayr, A. Moreo, and E. Dagotto, *ibid.* **71**, 014514 (2005).